Redox State of Pentraxin 3 as a Novel Biomarker for Resolution of Inflammation and Survival in Sepsis*

Friederike Cuello‡§¶, Manu Shankar-Hari‖, Ursula Mayr‡, Xiaoke Yin‡, Melanie Marshall‡, Gonca Suna‡, Peter Willeit‡‡§§, Sarah R. Langley‡, Tamani Jayawardhana‡, Tanja Zeller¶¶, Marius Terblanche‖, Ajay M. Shah‡, and Manuel Mayr‡‖‖**

In an endotoxaemic mouse model of sepsis, a tissue-based proteomics approach for biomarker discovery identified long pentraxin 3 (PTX3) as the lead candidate for inflamed myocardium. When the redox-sensitive oligomerization state of PTX3 was further investigated, PTX3 accumulated as an octamer as a result of disulfide-bond formation in heart, kidney, and lung—common organ dysfunctions seen in patients with sepsis. Oligomeric moieties of PTX3 were also detectable in circulation. The oligomerization state of PTX3 was quantified over the first 11 days in critically ill adult patients with sepsis. On admission day, there was no difference in the oligomerization state of PTX3 between survivors and non-survivors. From day 2 onward, the conversion of octameric to monomeric PTX3 was consistently associated with a greater survival after 28 days of follow-up. For example, by day 2 post-admission, octameric PTX3 was barely detectable in survivors, but it still constituted more than half of the total PTX3 in non-survivors ($p < 0.001$). Monomeric PTX3 was inversely associated with cardiac damage markers NT-proBNP and high-sensitivity troponin I and T. Relative to the conventional measurements of total PTX3 or NT-proBNP, the oligomerization of PTX3 was a superior predictor of disease outcome. ***Molecular & Cellular Proteomics 13: 10.1074/mcp.M114.039446, 2545–2557, 2014.***

Severe sepsis is a common acute illness in intensive care units (ICUs)[1] and is associated with high mortality rates and chronic morbidity. When it is associated with hypotension (termed septic shock), the mortality rate is very high (50% to 80%). Cardiovascular dysfunction during sepsis is multifactorial and often associated with minimal loss of myocardial tissue, but with the release of myocardial-specific markers such as troponins. A key unmet clinical need is the availability of a biomarker that predicts myocardial dysfunction early, monitors response to treatment, and thus identifies a cohort of patients at higher risk of septic shock to aid in targeted interventions and improve outcome (1).

In the present study, we used proteomics for biomarker discovery. Over the past decade, the field of proteomics has made impressive progress. Plasma and serum, however, are the most complex proteomes of the human body (2), and less abundant proteins tend to be missed in untargeted proteomics analyses of body fluids (3). Thus, we pursued an alternative strategy: the application of proteomics to diseased tissue (4), in which the potential biomarkers are less dilute and have a less uncertain cellular origin (5–7). We employed a solubility-based protein-subfractionation methodology to analyze inflammatory proteins that are retained with sepsis tissue. This innovative proteomics approach shall reveal inflammatory molecules that reside and persist within inflamed tissue. We hypothesized that proteins that accumulate in the susceptible tissues are more likely to be biomarker candidates for organ dysfunction than proteins that just circulate in plasma or serum. We then validated our proteomics findings in the preclinical model using samples from sepsis patients admitted to ICUs.

From the ‡King's British Heart Foundation Centre, King's College London, SE5 9NU London, UK; §Department of Experimental Pharmacology and Toxicology, Cardiovascular Research Centre, University Medical Center Hamburg-Eppendorf, Hamburg, 20246 Germany; ¶DZHK (German Center for Cardiovascular Research), partner site Hamburg/Kiel/Lübeck, Germany; ‖Critical Care Medicine, Guy's and St Thomas' NHS Foundation Trust, London, SE1 7EH UK; **Division of Asthma Allergy and Lung Biology, King's College, London SE1 9RT, UK; ‡‡Department of Public Health and Primary Care, University of Cambridge, Cambridge CB1 8RN, UK; §§Department of Neurology, Innsbruck Medical University, Innsbruck, 6020 Austria; ¶¶Clinic for General and Interventional Cardiology, University Heart Centre Hamburg, Hamburg 20246, Germany

Received March 13, 2014, and in revised form, June 1, 2014
Published, MCP Papers in Press, June 23, 2014, DOI 10.1074/mcp.M114.039446
Author contributions: M.S., M.T., A.M.S., and M. Mayr designed research; F.C., U.M., X.Y., M. Marshall, G.S., T.J., and T.Z. performed research; M.S., P.W., S.R.L., and M. Mayr analyzed data; F.C., M.T., A.M.S., and M. Mayr wrote the paper.

[1] The abbreviations used are: ICU, intensive care unit; AOF, acute organ failure; AUROC, area under the receiver operating characteristic curve; LPS, lipopolysaccharide; NT-proBNP, N-terminal of the prohormone brain natriuretic peptide; PTX3, pentraxin 3.

EXPERIMENTAL PROCEDURES

Materials—Antibodies recognizing pentraxin 3 (PTX3) were from Epitomics, Burlingame, CA (now Abcam, Cambridge, UK), α-actinin was from Sigma, cardiac myosin-binding protein C was a kind gift from Prof. Mathias Gautel from King's College London, telethonin was from Santa Cruz Biotechnology, Dallas, TX, and GAPDH conjugated to horseradish peroxidase (HRP) was from Abcam. All other chemicals were from Calbiochem, Invitrogen, Sigma-Aldrich, or VWR International, Lutterworth, Leicestershire, UK, unless otherwise stated. Male C57BL/6J mice were obtained from B&K Universal Ltd, Grimston, Aldbrough, Hull, UK.

Animal Models—All experiments were performed in accordance with UK Home Office regulations, and the investigation conformed with the Guide for the Care and Use of Laboratory Animals published by the U.S. National Institutes of Health (NIH Publication No. 85–23, revised 1996). The mouse model employed in this study was one of moderate-severity endotoxemia and has been characterized in detail previously (8, 9). In this model, there is significant hypotension with an approximately 25% to 30% decrease in systolic blood pressure at 12 to 18 h after lipopolysaccharide (LPS) injection. This is associated with significant cardiac dysfunction as assessed via *in vivo* volume loading protocols (8) or in terms of *ex vivo* cardiac myocyte contraction (9). Mortality is ~10% at this stage. C57/BL6 mice were injected intraperitoneally with 9 mg/kg *Escherichia coli* bacterial LPS (serotype 0.11:B4, Sigma Aldrich, UK). Control animals received intraperitoneal injections with an equivalent volume of saline. Mice were sacrificed 6 to 8 or 16 to 18 h after injection (9). Proteomics was performed 16 to 18 h post-injection, and immunoblot analysis was performed at both an early (6 to 8 h) and a late time point (16 to 18 h).

Immunohistochemical Analysis—Tissue was post-fixed in 4% formaldehyde, processed to paraffin blocks using an ASP300S dehydration machine (Leica, Wetzlar, Germany) and an EG1160 tissue-embedding system (Leica), and cut into 4-μm-thick slices. Sections were stained using a Ventana Benchmark XT machine (Ventana, Tuscon, AZ). Deparaffinized sections were incubated for 60 min in CC1 solution (Ventana) for antigen retrieval. Primary antibodies were diluted in 5% goat serum (Dianova, Hamburg, Germany), 45% Tris-buffered saline, pH 7.6, and 0.1% Triton X-100 in antibody diluent solution (Zytomed, Berlin, Germany). Sections were then incubated with primary antibody against Iba1 (Wako Chemicals, Neuss, Germany, 1:2000), Ly6G (eBiosciences, San Diego, CA, 1:2000), or PTX3 (TNFAIP5 polyclonal, HRP conjugated, 1:100) for 60 min. Histofine Simple Stain MAX PO Universal immunoperoxidase polymer purchased from Nichirei Biosciences (Wedel, Germany) was used as secondary antibody. Detection of secondary antibodies was performed with an Ultraview Universal DAB detection kit from Ventana. Counterstaining was performed using Ventana's hematoxylin solution. Sections were coverslipped using TissueTek glove mounting medium (Sakura Finetek, Staufen, Germany) and dried in an incubator at 60 °C.

Subfractionation of Mouse Hearts—Mouse heart homogenates were subfractionated into Triton-soluble and Triton-insoluble fractions. Briefly, 1% (v/v) Triton X-100 was added to the mouse heart homogenates, which were then incubated for 15 min on a shaking platform at 4 °C and centrifuged at 13,000*g* for 5 min (4 °C). The Triton-soluble fraction was separated from the Triton-insoluble fraction, and non-reducing Laemmli sample buffer was added.

Proteomics Analysis—The Triton-insoluble fractions from control ($n = 4$) and septic ($n = 4$) groups were denatured in Laemmli buffer at 97 °C for 5 min. The proteins were separated by 5–20% gradient Tris-glycine gel at 5 W for 45 min and then 30 W for 4.5 h. After electrophoresis, gels were stained using the PlusOne Silver Staining Kit (GE Healthcare). Silver staining was used for band staining to avoid cross-contamination with fainter gel bands. All gel bands ($n = 48$ per sample) were excised in identical parallel positions across lanes, and no empty gel pieces were left behind. Subsequently, all gel bands were subjected to in-gel tryptic digestion using an Investigator ProGest (Digilab, Marlborough, MA) robotic digestion system. Tryptic peptides were separated on a nanoflow LC system (Dionex Ultimate 3000, Thermo Fisher Scientific) using reversed phase columns (PepMap C18, 25 cm $\times$ 75 μm) and eluted with a 40-min gradient (10% to 25% B in 35 min, 25% to 40% B in 5 min, 90% B in 10 min, and 2% B in 20 min, where A was 2% acetonitrile, 0.1% formic acid in HPLC H_2O and B was 90% acetonitrile, 0.1% formic acid in HPLC H_2O). Sequentially eluted peptides were directly analyzed via tandem mass spectrometry (LTQ Orbitrap XL, Thermo Fisher Scientific) using full ion scan mode over the mass-to-charge (*m/z*) range of 450–1600. Tandem MS (MS/MS) was performed on the top six ions using the data-dependent mode with dynamic exclusion (10, 11). Peak lists were generated using extract_msn_com.exe (version 5.0, Thermo Fisher Scientific) and searched against the UniProt/Swiss-Prot mouse database (version 2014_01, 16,656 protein entries) using Mascot (version 2.3.01, Matrix Science, Boston, MA). The mass tolerance was set at 30 ppm for the precursor ions and at 0.8 Da for fragment ions. Carboxyamidomethylation of cysteine was used as a fixed modification, and oxidation of methionine as a variable modification. Two missed cleavages were allowed. Scaffold (version 4.3.0, Proteome Software Inc., Portland, OR) was used to calculate the normalized spectral counts and to validate peptide and protein identifications. According to the default values in the Scaffold software, peptide identifications were accepted if they could be established at greater than 95% probability as specified by the Peptide Prophet algorithm. Only tryptic peptides were included in the analysis. Protein identifications were accepted if they could be established at greater than 99% probability with at least two independent peptides.

Proteomic Differential Expression Analysis—Proteomic differential expression was assessed using the normalized spectral abundance factor power-law global error model (12). The normalized spectral abundance factor was calculated for each protein detected. Spectral count values of 0 were replaced by an empirically derived fractional value. The value was calculated to be the smallest value between 0 and 1, which provided the best fit to a normal distribution, as determined by a Shapiro–Wilks test. The normalized spectral abundance factor values were fit to a power-law global error model; differentially expressed proteins were then identified through a signal-to-noise (STN) test statistic. Proteins were kept for further analysis if spectra were detected in at least two samples per group or if spectra were detected in all samples of one group and were absent in all samples of the other group. The false discovery rate was estimated by comparing the signal-to-noise statistic to an empirically derived null distribution using the resampling procedure described by Pavelka *et al.* and implemented in the plgem R package (13).

Preparation of Tissue Homogenates—Control and septic hearts or other tissues (aorta, kidney, spleen, liver, lung, muscle, brain) were excised and washed briefly in ice-cold Tyrode's solution (pH 7.4) containing in 130 mM NaCl, 5.4 mM KCl, 1.4 mM $MgCl_2$, 0.4 mM NaH_2PO_4, and 4.2 mM HEPES to remove blood. The tissue was snap-frozen in liquid nitrogen before homogenization using a motor-driven blade "on ice" in a Tris-based homogenization buffer (pH 7.4) containing 100 mM Tris/HCl, 100 mM EDTA, 100 mM maleimide, and protease inhibitors (Roche) at a ratio of 100 mg/ml (10%). Laemmli sample buffer with 10% β-mercaptoethanol (reducing) or 100 mM maleimide (non-reducing) was added to the tissue homogenates, and samples were passed through a narrow-gauge needle to shear DNA.

Preparation of Mouse Plasma Samples—Whole mouse blood from control or LPS-treated mice was collected, and 2 mM EDTA was added. The samples were centrifuged for 15 min at 2000*g* at 4 °C to

deplete cells. Non-reducing Laemmli sample buffer was added to the resulting plasma supernatant.

SDS-PAGE and Immunoblot Analysis—Protein samples from tissue homogenates, fractionated homogenates, or plasma samples in reducing or non-reducing Laemmli sample buffer were separated via 7.5%, 10%, or 15% SDS-PAGE, transferred to polyvinylidene difluoride membranes, and subjected to immunoblotting. Primary antibodies were detected by donkey anti-rabbit or sheep anti-mouse secondary antibodies linked to HRP (GE Healthcare). Specific protein bands were detected via enhanced chemiluminescence (GE Healthcare) and quantified on a calibrated densitometer (GS-800, Bio-Rad) using Quantity One® one-dimensional analysis software (v. 4.5.1).

Fluorescence Immunohistochemical Staining—Mouse hearts were prepared as described above. For antigen retrieval, deparaffinized sections were boiled for 60 min in 10 mM citrate buffer (10 mM sodium citrate, 0.05% Tween-20, pH 6.0) using a steamer. Afterward, sections were blocked for 60 min in PBS containing donkey serum (1.2 mg/ml; Dianova) and then with 1% Sudan black in 70% ethanol for 20 min in order to decrease autofluorescence of the tissue. After rigorous washing, sections were incubated with anti-PTX3 (1:100; Abcam, Cambridge, UK) primary antibody overnight at 4 °C. Sections were then washed again, and secondary donkey anti-rabbit IgG Alexa 633 labeled antibody (1:200; Invitrogen, Darmstadt, Germany) was applied for 60 min. Nuclei were counterstained by 0.4 μg/ml 4′6-diamidino-2′-phenylindole (DAPI) (Roche, Munich, Germany) in PBS for 10 min, and slides were mounted in Fluoromount G (Biozol, Munich, Germany). Images were taken on a fluorescence light microscope equipped with a digital camera (Axio Imager M2, Zeiss, Jena, Germany).

Study Population—An observational cohort study was performed in an 88-bed university hospital general medical-surgical ICU. The study protocol received ethical approval from an institutional review board (REC reference 12/LO/0326); written informed consent was obtained either from the patient, if mentally competent, or from the next of kin, and the consent procedure was completed with retrospective consent. The clinical management of the patient was at the discretion of the attending physicians. The investigators analyzing samples were blinded to patients' outcomes while conducting the experiments. Consecutive patients meeting the definition for severe sepsis within the first 12 h following ICU admission between May and October 2011 were included. Severe sepsis was defined as evidence of two or more systemic inflammatory response syndrome criteria, with proven or suspected infection and at least one organ system dysfunction (cardiovascular, respiratory, renal, hematological, or metabolic) (14). Organ function was classified and categorized using the sequential organ failure assessment score. Exclusion criteria included patients younger than 18 years, those with congenital hypogammaglobulinemia, known protein-losing enteropathies, nephrotic syndrome, neoplastic or proliferative hematological diseases, those having received intravenous immunoglobulins in the past 3 months, those receiving high-dose steroid therapy, those having other ongoing immune dysfunction as defined by the APACHE II co-morbidities, ongoing blood loss (defined by a blood transfusion requirement of >2 units/24-h period), and retroviral disease. Blood samples for measurements were obtained daily from day 0 (ICU admission) until day 6 and at day 11. Whole blood from septic patients was collected at the indicated time points; the blood was allowed to clot by being left undisturbed at room temperature for 15 to 30 min. The clot was removed by centrifugation at 2000*g* for 10 min at 4 °C. Following centrifugation, the serum was immediately transferred into a clean polypropylene tube and stored at −80 °C. For immunoblotting, serum samples were incubated with Blue Sepharose® CL-6B (50 μl per 200 μl of serum) at 4 °C for 1 h on a shaking platform to deplete from serum albumin. Samples were centrifuged at 1000*g* for 1 min at 4 °C to remove Blue Sepharose® CL-6B beads, non-reducing Laemmli sample buffer was added, and equal volumes of depleted samples were analyzed via Western immunoblot analysis.

Immunoassays—NT-proBNP and high-sensitivity troponin T were determined via the electrochemiluminescence sandwich immunoassay ECLIA on an Elecsys 2010 system (Roche Diagnostics, Germany) in serum samples according to the manufacturers' recommendations. The assay range for NT-proBNP was 5 to 35,000 pg/ml, the assay range for high-sensitivity troponin T was 3 to 10,000 pg/ml. High-sensitivity troponin I was determined by means of cardiac troponin assay (ARCHITECT STAT highly sensitive Troponin I immunoassay on an ARCHITECT i2000SR, Abbott Diagnostics). The established limit of detection for the assay ranges from 0.8 to 1.9 with a median of 1.5 pg/ml and an assay range of 0–50,000 pg/ml. Human Pentraxin 3/TSG-14 was measured in 28 participants, including all non-surivivors, with a Quantikine ELISA Kit from R&D Systems, Minneapolis, MN.

Statistics—Monomeric, tetrameric, and octameric PTX3 levels in patients admitted to the ICU were not normally distributed. We therefore used the median and interquartile range to summarize their distributions and used the Wilcoxon rank-sum test to formally test for differences between participants who survived the 28-day follow-up period and those who did not. Analogous methods were used for the biomarkers NT-proBNP, high-sensitivity troponin T, and high-sensitivity troponin I. Analyses were performed using Stata release 12.1 (StataCorp, College Station, TX). Statistical tests were two-sided and used a significance level of $p < 0.05$.

RESULTS

Biomarker Discovery in a Preclincial Model—For our proteomic investigation, we chose the mouse model of endotoxemia to identify biomarker candidates. As organs susceptible to sepsis-induced dysfunction, hearts were isolated from control or septic mice 16 to 18 h after the injection of vehicle saline solution or LPS (9 mg/kg intraperitoneal) (9). Before proteomics, all tissue specimens were examined histologically. Macrophage and neutrophil infiltration was detected via immunostaining within 6 to 8 h after LPS injection. Representative images are shown in Fig. 1*A*. Hearts were obtained from control and LPS-treated mice ($n = 4$ per group). To enable a better characterization of inflammatory proteins retained within the cardiac tissue, we used a solubility-based protein subfractionation methodology based on 1% Triton. The Triton-insoluble protein extracts were separated via SDS-PAGE (supplemental Fig. S1), subjected to in-gel tryptic digestion, and analyzed via LC-MS/MS using a high-mass-accuracy ion trap (LTQ-Orbitrap XL, Thermo Fisher Scientific). The entire MS/MS dataset has been deposited to the ProteomeXchange Consortium via the PRIDE partner repository with the dataset identifier PXD001020 and DOI 10.6019/PXD001020 (www.ebi.ac.uk/pride/). Only proteins passing stringent identification criteria are listed in supplemental Table S1 ($n = 1910$). The identified peptides corresponding to these protein identifications are given in supplemental Table S2. According to the Gene Ontology Annotation database, 66 non-redundant proteins were secreted proteins in the Triton-insoluble fraction. Differences in relative protein abundance between control and LPS-treated hearts were estimated using normalized spectral counts (Table I). No outliers were removed. Details

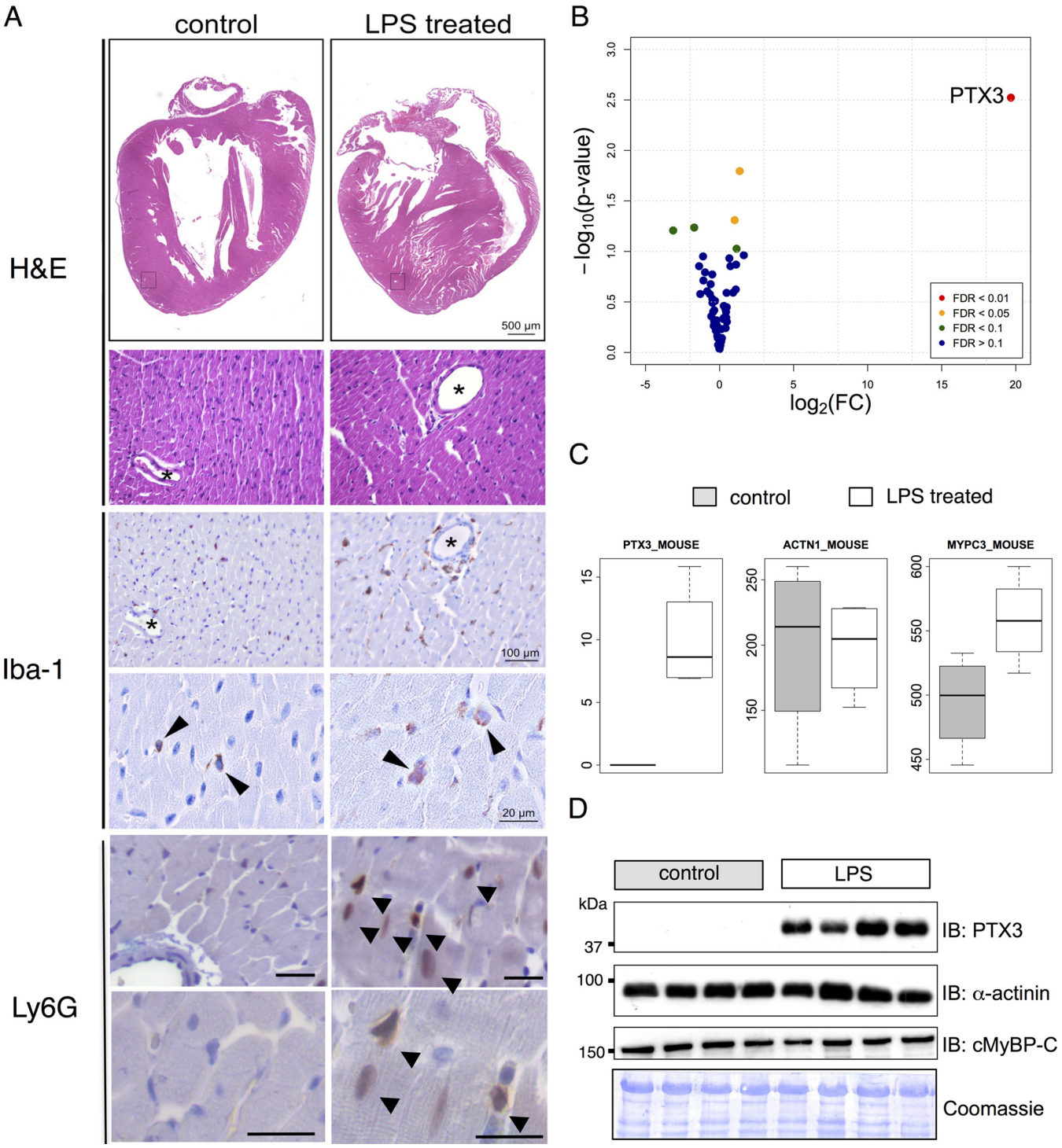

FIG. 1. **Proteomics in a preclinical model of sepsis.** *A*, hematoxylin and eosin (H&E) staining of hearts from control C57Bl6 and LPS-treated mice. Immunostaining for the macrophage marker ionized calcium binding adaptor molecule 1 (Iba-1) and the granulocyte marker Ly6G. *B*, differential expression in the proteomic analysis. Note the pronounced up-regulation of pentraxin 3 (PTX3) in the Triton-insoluble fraction of LPS-treated hearts. *C*, comparative quantification for PTX3 via mass spectrometry; equal expression of α-actinin-1 (ACTN1 MOUSE) and cardiac myosin-binding protein C (MYPC3 MOUSE). *D*, representative immunoblots of the Triton-insoluble fraction performed on four hearts per group. Probing for α-actinin, cardiac myosin-binding protein C (cMyBP-C), and Coomassie staining assured equal protein loading.

TABLE I
Extracellular/secreted proteins identified via proteomics in the Triton-insoluble fraction of cardiac tissue

Protein name	Swiss-Prot accession	Control[a] (mean spectra ± S.D.)	LPS[a] (mean spectra ± S.D.)	Log fold change	False discovery rate
Pentraxin-related protein PTX3	PTX3_MOUSE	0 ± 0	10 ± 4	19.67	0.003[b]
Galectin-1	LEG1_MOUSE	8 ± 3	22 ± 4	1.36	0.016[b]
Thioredoxin	THIO_MOUSE	4 ± 5	9 ± 5	1.02	0.049[b]
von Willebrand factor A domain-containing protein 1	VWA1_MOUSE	6 ± 1	2 ± 2	−1.71	0.058[b]
Versican	CSPG2_MOUSE	8 ± 16	1 ± 1	−3.14	0.062[b]
Inter-α-trypsin inhibitor heavy chain 4	ITIH4_MOUSE	3 ± 3	9 ± 7	1.51	0.078[b]
Vitronectin	VTNC_MOUSE	4 ± 3	8 ± 7	1.15	0.094[b]
Complement C3	CO3_MOUSE	2 ± 2	6 ± 4	1.64	0.109
Mimecan	MIME_MOUSE	5 ± 2	2 ± 2	−1.12	0.112
Prolargin	PRELP_MOUSE	18 ± 12	29 ± 10	0.66	0.117
Antithrombin-III	ANT3_MOUSE	2 ± 1	4 ± 3	1.12	0.135
Calmodulin	CALM_MOUSE	3 ± 4	5 ± 5	0.73	0.14
Reticulon-3	RTN3_MOUSE	4 ± 2	2 ± 2	−1.38	0.14
Complement C1q tumor necrosis factor related protein 9	C1QT9_MOUSE	4 ± 4	2 ± 2	−0.98	0.161
Dermatopontin	DERM_MOUSE	23 ± 6	16 ± 4	−0.49	0.169
Collagen α-1 (I)	CO1A1_MOUSE	6 ± 7	3 ± 4	−1.09	0.194
Laminin subunit β-2	LAMB2_MOUSE	54 ± 8	35 ± 14	−0.60	0.211
Collagen α-6 (VI)	CO6A6_MOUSE	2 ± 2	5 ± 2	1.09	0.238
Dystroglycan	DAG1_MOUSE	5 ± 1	3 ± 2	−0.84	0.248
Uncharacterized aarF domain containing protein kinase 1	ADCK1_MOUSE	1 ± 1	2 ± 2	0.91	0.256
Annexin A2	ANXA2_MOUSE	8 ± 2	12 ± 3	0.47	0.257
Laminin subunit α-5	LAMA5_MOUSE	4 ± 2	1 ± 2	−1.31	0.264
Collagen α-1 (XV)	COFA1_MOUSE	15 ± 2	10 ± 3	−0.66	0.265
Apolipoprotein A-I	APOA1_MOUSE	6 ± 3	4 ± 3	−0.49	0.295
Vinculin	VINC_MOUSE	131 ± 52	106 ± 8	−0.30	0.309
Translationally controlled tumor protein	TCTP_MOUSE	3 ± 4	2 ± 3	−0.48	0.323
Decorin	PGS2_MOUSE	25 ± 10	30 ± 6	0.28	0.346
Inter-α trypsin inhibitor heavy chain 1	ITIH1_MOUSE	6 ± 2	9 ± 3	0.48	0.356
Periostin	POSTN_MOUSE	11 ± 6	15 ± 6	0.40	0.367
Fibrinogen γ chain	FIBG_MOUSE	6 ± 3	8 ± 4	0.39	0.371
Cadherin-13	CAD13_MOUSE	19 ± 5	15 ± 3	−0.36	0.382
Clusterin	CLUS_MOUSE	3 ± 1	4 ± 4	0.44	0.396
Papilin	PPN_MOUSE	16 ± 7	12 ± 4	−0.43	0.396
Perlecan	PGBM_MOUSE	10 ± 4	7 ± 3	−0.56	0.439
Ceruloplasmin	CERU_MOUSE	3 ± 1	4 ± 3	0.45	0.452
Peroxidasin homolog	PXDN_MOUSE	5 ± 4	7 ± 4	0.44	0.452
Glutathione peroxidase 3	GPX3_MOUSE	5 ± 5	6 ± 2	0.27	0.456
Protein-glutamine γ-glutamyltransferase 2	TGM2_MOUSE	27 ± 2	31 ± 11	0.23	0.466
Collagen α-1 (VI)	CO6A1_MOUSE	84 ± 13	73 ± 22	−0.20	0.481
Galectin-9	LEG9-MOUSE	4 ± 1	3 ± 3	−0.34	0.482
EMILIN-1	EMIL1_MOUSE	15 ± 5	12 ± 4	−0.31	0.492
EGF-containing fibulin-like extracellular matrix protein 1	FBLN3_MOUSE	4 ± 2	3 ± 2	−0.37	0.492
Coatomer subunit α	COPA_MOUSE	2 ± 2	2 ± 3	0.49	0.497
Talin-1	TLN1_MOUSE	10 ± 3	7 ± 6	−0.38	0.537
Nidogen-1	NID1_MOUSE	88 ± 16	78 ± 8	−0.17	0.543
Filamin-A	FLNA_MOUSE	8 ± 7	6 ± 2	−0.39	0.546
Apolipoprotein O	APOO_MOUSE	13 ± 6	12 ± 6	−0.17	0.558
Dehydrogenase/reductase SDR family member 7C	DRS7C_MOUSE	21 ± 5	18 ± 5	−0.17	0.558
Gelsolin	GELS_MOUSE	5 ± 2	4 ± 2	−0.29	0.565
Fibronectin	FINC_MOUSE	2 ± 1	3 ± 2	0.41	0.574
Apolipoprotein O-like	APOOL_MOUSE	23 ± 8	25 ± 11	0.13	0.588
von Willebrand factor A domain-containing protein 8	VWA8_MOUSE	14 ± 3	12 ± 9	−0.25	0.608
Asporin	ASPN_MOUSE	5 ± 5	5 ± 3	−0.15	0.687
Collagen α-2 (VI)	CO6A2_MOUSE	47 ± 4	44 ± 10	−0.10	0.708
Laminin subunit γ-1	LAMC1_MOUSE	35 ± 12	32 ± 4	−0.12	0.721
Protein disulfide-isomerase	PDIA1_MOUSE	2 ± 2	3 ± 1	0.16	0.721

TABLE I—*continued*

Protein name	Swiss-Prot accession	Control[a] (mean spectra ± S.D.)	LPS[a] (mean spectra ± S.D.)	Log fold change	False discovery rate
Transforming growth factor-β-induced protein ig-h3	BGH3_MOUSE	9 ± 3	10 ± 1	0.12	0.721
Nidogen-2	NID2_MOUSe	10 ± 7	10 ± 3	0.13	0.74
Lumican	LUM_MOUSE	26 ± 8	28 ± 9	0.06	0.764
Tubulointerstitial nephritis antigen-like	TINAL_MOUSE	10 ± 4	11 ± 4	0.08	0.767
Fibulin-5	FBLN5_MOUSE	2 ± 3	3 ± 2	0.11	0.779
Laminin subunit β-1	LAMB1_MOUSE	22 ± 8	23 ± 6	0.08	0.789
Plasminogen	PLMN_MOUSE	2 ± 2	1 ± 0	−0.10	0.842
Fibromodulin	FMOD_MOUSE	2 ± 3	2 ± 3	0.06	0.845
Fibrinogen β chain	FIBB_MOUSE	6 ± 4	6 ± 2	0.02	0.882
Matrin-3	MATR3_MOUSE	8 ± 3	8 ± 3	−0.02	0.913
Laminin subunit α-2	LAMA2_MOUSE	46 ± 10	46 ± 7	0.00	0.924

[a] Four biological samples analyzed per group ($n = 4$).
[b] Indicates proteins with a false discovery rate ≤ 0.1.

can be found in "Experimental Procedures." Long PTX3 was returned as the most pronounced change (Fig. 1*B*). PTX3 is an acute-phase glycoprotein secreted in response to proinflammatory cytokines (15). The quantitative difference according to the proteomics data (Fig. 1*C*) was validated by immunoblotting. Immunblots confirmed a marked increase of PTX3 in the Triton-insoluble cardiac extracts under endotoxemic conditions (Fig. 1*D*). Equal protein loading was demonstrated by immunoblotting for the sarcomeric proteins α-actinin and cardiac myosin-binding protein C, and by Coomassie staining.

Redox-dependent Oligomerization of PTX3—Oligomerization of PTX3 into tetrameric and octameric complexes via interprotein disulfide-bond formation through adjacent cysteine residues in PTX3 monomer subunits was described as a prerequisite for its biological activity and binding to constituents of the extracellular matrix (16). To further investigate the enrichment of PTX3 in septic hearts, the Triton-soluble and Triton-insoluble fractions were compared under reducing and non-reducing conditions 6 to 8 h post–LPS injection ($n = 3$ per group). The effectiveness of subfractionation by 1% Triton was confirmed by immunoblotting for selected markers of different cardiomyocyte compartments, glyceraldehyde-3-phosphate dehydrogenase (GAPDH) (cytosolic) and telethonin (particulate/myofilament) (Fig. 2*A*). Under reducing conditions, PTX3 was clearly detectable as a 45-kDa moiety in sepsis hearts (Fig. 2*A*, upper panel). *N*-linked glycosylation accounts for a 5-kDa shift of PTX3 with a predicted molecular mass for the reduced protein of 40 kDa (17). Immunoblot analysis performed under non-denaturing conditions revealed that PTX3 formed high-molecular-weight complexes resulting in the formation of tetramers (180 kDa) and octamers (360 kDa) (Fig. 2*A*, lower panel) in response to oxidant exposure. Although both the tetramer and the octamer were present in the Triton-soluble fraction, only the octamer was detectable in the Triton-insoluble fraction of septic hearts. Next, we tested different tissue homogenates. Interestingly, there was a preponderance of the oxidized *versus* the reduced form of PTX3, with oxidized PTX3 accumulating in the heart, aorta, kidney, and lung—organs that are known to be susceptible to septic complications (Fig. 2*B*, upper and lower panels). Less oxidized PTX3 was retained in the spleen and liver. This is consistent with previous reports that LPS induces PTX3 expression *in vivo* in heart and lung but not in liver (18, 19). The high-molecular-weight PTX3 moieties were converted to monomers under reducing conditions. In contrast, no PTX3 protein was detectable in tissue homogenates of control mice. Notably, the immunoblots presented in Fig. 2*C* highlight bands consistent with the expected molecular weights of tetrameric and octameric moieties of PTX3 in plasma of septic mice. PTX3 can be expressed by a variety of cells in response to LPS and inflammatory cytokines (20, 21). Positive immunostaining for PTX3 in the heart was predominantly observed in the vicinity of smaller vessels (Fig. 3) at sites of leukocyte and macrophage infiltration (supplemental Fig. S2). Besides PTX3, known first- and second-degree interaction partners of PTX3 were identified in the proteomics screen (Fig. 4).

Circulating PTX3 in Sepsis Patients—PTX3 is barely detectable in the plasma of healthy individuals (<2 ng/ml), but its concentration can increase to up to 200 ng/ml in sepsis, depending on the severity of the disease (22). High PTX3 plasma levels are correlated with severity of infection in patients with sepsis or septic shock (23–25). Based on our findings in the preclinical model, we quantified octameric, tetrameric, and monomeric PTX3 levels in critically ill patients with sepsis but without established acute organ failure (AOF) referred to ICU Outreach Teams ($n = 31$). Their clinical characteristics are shown in Table II. Samples were taken in a longitudinal manner at eight different time points: on the day of admission to ICU (day 0), at days 1 through 6, and at day 11. Immunoblot analysis was performed under non-reducing conditions in a total of 204 samples (Fig. 5*A*). Next, we tested to see whether the levels of the different oligomeric PTX3 moieties could be used to distinguish survivors from non-survivors. On day 0, there was no difference in octameric,

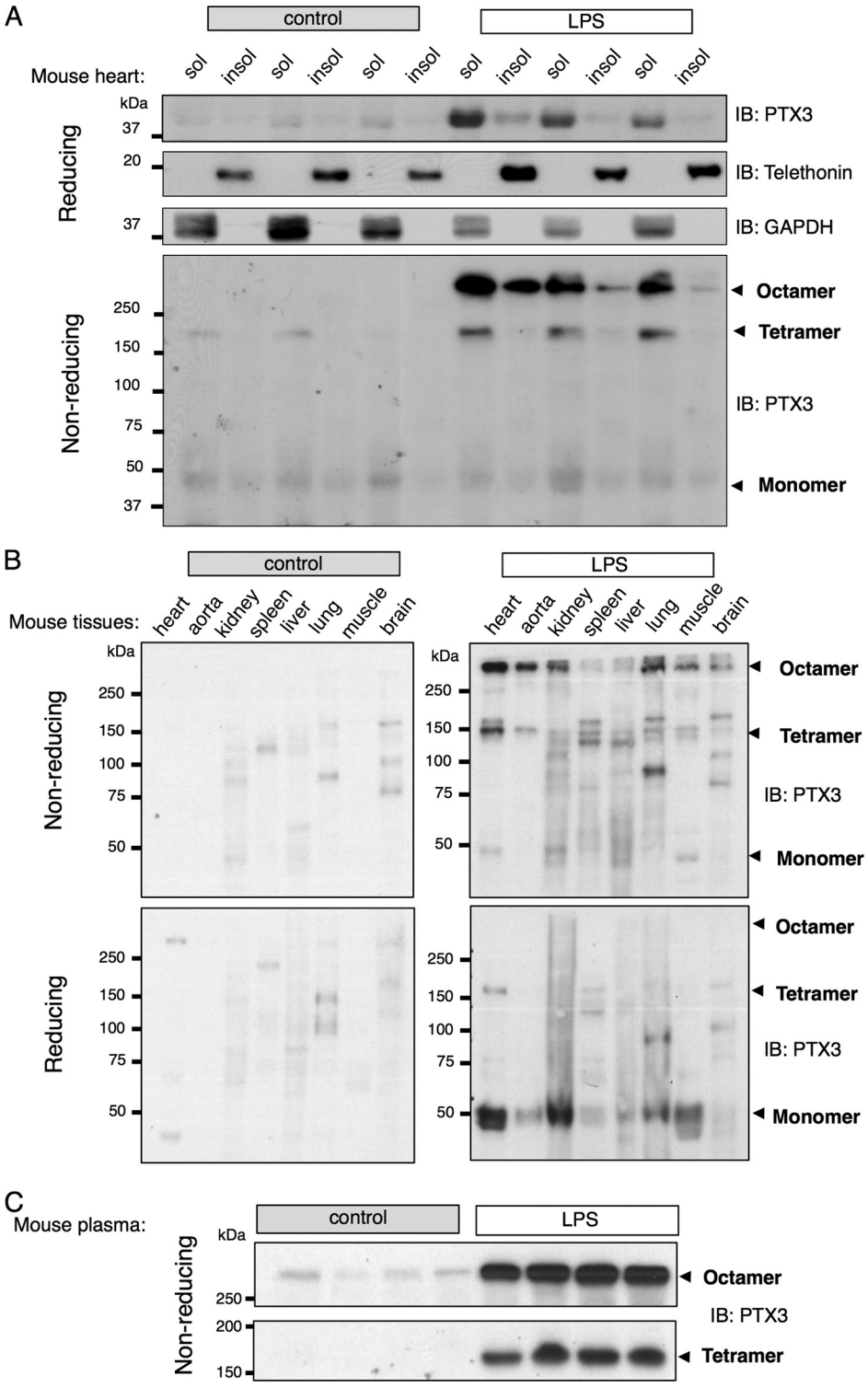

FIG. 2. **Redox state of PTX3 in endotoxemia.** *A*, the different oxidation states of PTX3 in the heart (octamer, tetramer, and monomer) were visualized in the Triton-soluble (sol) and -insoluble (insol) fractions under reducing (upper panel) or non-reducing conditions (bottom panel). Representative immunoblots from three mouse hearts per group were probed for PTX3, telethonin (marker of the insoluble myofilament-containing compartment), and GAPDH (marker of the soluble cytosol-containing compartment). *B*, tissue samples from heart, aorta, kidney, spleen, liver, lung, muscle, and brain were subjected to immunoblot analysis under non-reducing (upper panel) or reducing (bottom panel) gel conditions and probed for PTX3. *C*, plasma samples from control C57Bl6 and LPS-treated mice were depleted of albumin and analyzed for PTX3 protein content and oxidation state using immunoblot analysis under non-reducing conditions. The representative immunoblots display the results of four mice per group.

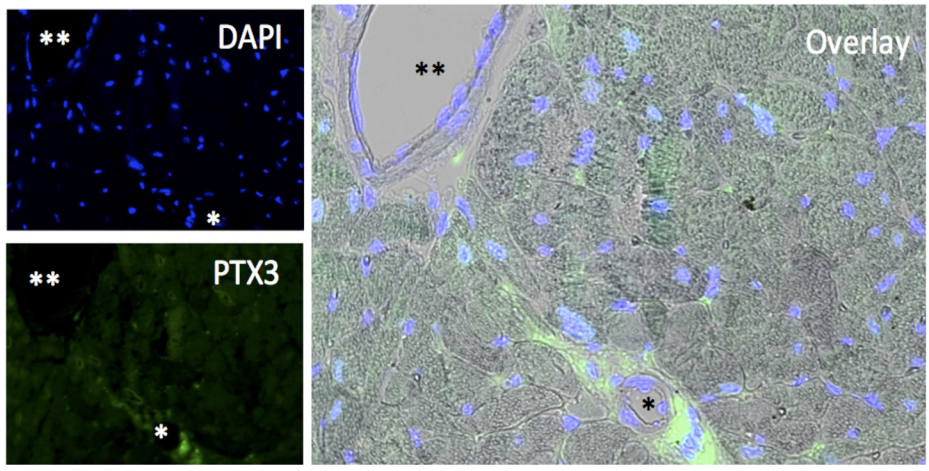

FIG. 3. **Localization of PTX3.** Immunofluorescence staining for PTX3. Perivascular localization of PTX3 (green) in hearts from LPS-treated mice. Nuclear counterstaining with DAPI (blue).

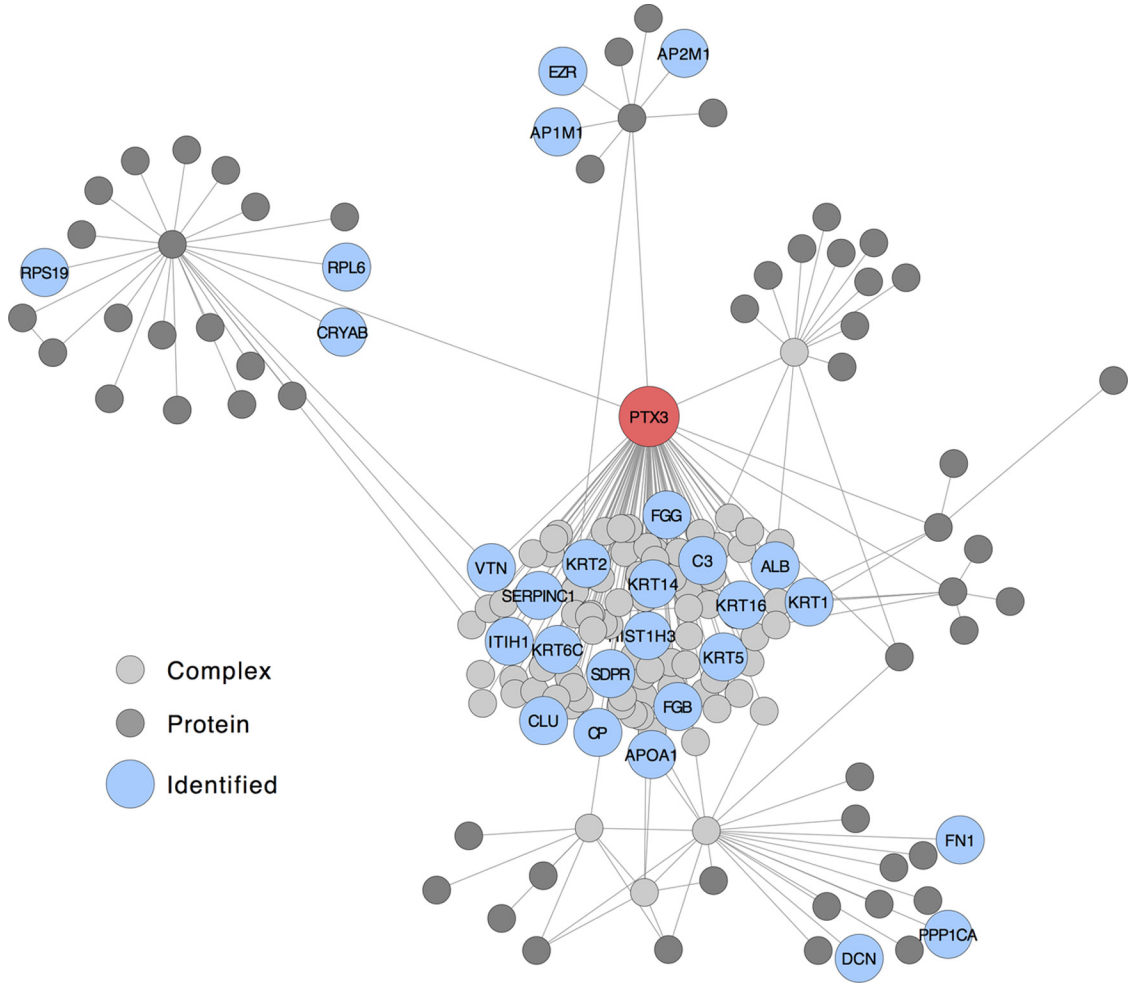

FIG. 4. **Protein interactions of PTX3.** Protein interactions of PTX3, from Innate DB, are shown with PTX3 in red. The dark gray nodes are the first and second-degree interaction proteins from PTX3; the light gray nodes are proteins that form a complex that interacts with PTX3. Abbreviations are given as Gene ID (Human). The large nodes in blue are proteins identified by proteomics (supplemental Table S1).

tetrameric, and monomeric PTX3 levels between survivors and non-survivors. Over the time course of 11 days, however, the transformation of octameric to monomeric PTX3 was associated with greater survival during 28-day follow-up (Fig. 5*B*). As early as day 2 post-admission, PTX3 oligomerization predicted adverse clinical outcome: Octameric PTX3 was barely detectable in survivors but constituted more than 50% of total PTX3 in non-survivors ($p < 0.001$; Fig. 5*C*). In contrast,

TABLE II
Clinical characteristics of sepsis patients

Variable[a]	Entire study cohort ($n = 31$)	28-day survivors ($n = 23$)	28-day non-survivors ($n = 8$)	p value[b]
Age (years)	67.4 ± 11.9	66.0 ± 12.2	71.0 ± 12.8	0.29
Male:female, *n* (%)	19:12 (61.3%:38.3%)	15:8 (65.3%:34.7%)	4:4 (50.0%:50.0%)	0.45
APACHE II score	20.6 ± 6.0	19.3 ± 6.1	24.4 ± 3.7	0.03
Medical:surgical, *n*	26:5 (83.8%:16.1%)	18:5 (78.3%:21.7%)	8 (100%)	0.20
WCC ($\times 10^9$/l)	13.5 (1.3, 49.1)	11.3 (1.3, 25.8)	17.8 (11.8, 49.1)	0.04
CRP (mg/l)	130 (8, 429)	143 (8, 429)	115 (29, 148)	0.13
CVS SOFA score	4 (0, 4)	4 (0, 4)	4 (0, 4)	0.47
Renal SOFA score	1 (0, 4)	1 (0, 4)	0 (0, 4)	0.50
t-SOFA score	8 (4, 12)	8 (2, 14)	8 (3, 13)	0.98
RRT, *n*	5	4	1	0.77
ICU LOS (days)	9.9 ± 5.7	9.5 ± 6.3	11 ± 3.5	0.23
Hospital LOS (days)	23 (4, 216)	30 (7, 216)	11 (4, 18)	0.001

APACHE, Acute Physiology and Chronic Health Evaluation II; WCC, white cell count; CRP, C-reactive protein; CVS SOFA, cardiovascular sequential organ failure assessment; t-SOFA, total sequential organ failure assessment; RRT, renal replacement therapy; LOS, length of stay.
[a] Values presented are unadjusted means ± S.D., range (min, max), or percentages.
[b] p values were calculated via t test (continuous variables) or the χ^2 test (categorical variables).

monomeric PTX3 constituted 90% of total PTX3 in survivors but only 20% in non-survivors ($p < 0.013$). There was no significant difference in tetrameric PTX3 between survivors and non-survivors.

Comparison to Established Biomarkers—Secreted PTX3 can bind to pathogens to induce classical complement activation (20). Notably, monomer levels of PTX3 were inversely correlated to complement C3a ($r_s = -0.455$, $n = 24$, $p = 0.014$), as well as the cardiac and stress markers high-sensitivity troponin I ($r_s = -0.565$, $n = 28$, $p = 0.001$), high-sensitivity troponin T ($r_s = -0.358$, $n = 28$, $p = 0.067$), and N-terminal pro-B-type natriuretic peptide ($r_s = -0.352$, $n = 28$, NT-proBNP, $p = 0.066$) (supplemental Fig. S3*A*), suggesting that the absence of oligomerization is associated with less complement activation and less cardiac tissue damage. Patients with the maximum cardiovascular sequential organ failure assessment score ($n = 19$) at day 1 post-admission to ICU had on average 4-fold higher oligomerized PTX3 levels than patients with a lower cardiovascular sequential organ failure assessment score ($n = 12$) (oligomerized PTX3, density in arbitrary units, mean ± S.E.: 1.38 ± 0.40 *versus* 0.31 ± 0.18, $p = 0.022$). Unlike oligomerized PTX3 moieties, the cardiac damage markers were not significantly correlated with the survival of patients (supplemental Fig. S3*B*). Octameric and monomeric PTX3 levels at day 2 predicted the 28-day survival better than a model containing total PTX3 as measured by conventional ELISA (AUROC: 0.918 *versus* 0.626; p value: 0.045; Fig. 6*A*) or NT-proBNP (AUROC: 0.918 *versus* 0.687; p value: 0.023; Fig. 6*B*), a marker for left ventricular dysfunction that is frequently increased in severe sepsis (26). Although octameric to monomeric PTX3 was superior to total PTX3 and NT-proBNP, this single biomarker did not outperform the APACHE II score related risk prediction (AUROC 0.918 *versus* 0.803, $p = 0.25$), which includes clinical variables and organ dysfunction biochemistry and accounts for co-morbidities (27).

DISCUSSION

Our study provides proof-of-principle data that the oligomerization state of PTX3 may represent a superior prognostic marker relative to total PTX3 in adult critically ill patients with severe sepsis. This distinction between the oligomerization state of PTX3 and conventional measurements of total PTX3 is important, as the oligomerization state might better mirror the changes in the underlying complex interactions between immune-inflammatory insults and redox stress in sepsis. Furthermore, key strengths of our study are the bridging of proteomics discovery to bedside validation and the direct comparison to established biomarkers, which directly addresses the main criticisms often highlighted in proteomics biomarker research.

Role of PTX3—Together with C-reactive protein and serum amyloid P component, PTX3 belongs to the family of pentraxins. Although C-reactive protein is used as a marker of systemic inflammation, its prognostic value in sepsis is poor (28). PTX3 plays an important role in regulating the innate immune response by contributing to opsonization (29). In mice, overexpression of PTX3 confers resistance to the lethal effects of LPS (30). LPS injection elicits the secretion of several cytokines, including interleukin-1 and tumor necrosis factor α, two potent inducers of PTX3. Unlike the classical pentraxins C-reactive protein and serum amyloid P component, PTX3 does not bind phosphoethanolamine or phosphocholine, but it does bind collagen-like C1q, the first component of the classical pathway of complement activation. Its capacity to bind C1q is mediated by the pentraxin domain and requires multimer formation (17). Thus, PTX3 oligomers may reflect activity better than total PTX3 as measured by ELISA. As expected on the basis of C1q binding, high PTX3 may cause the consumption of C4 and of the total complement hemolytic activity in serum (17).

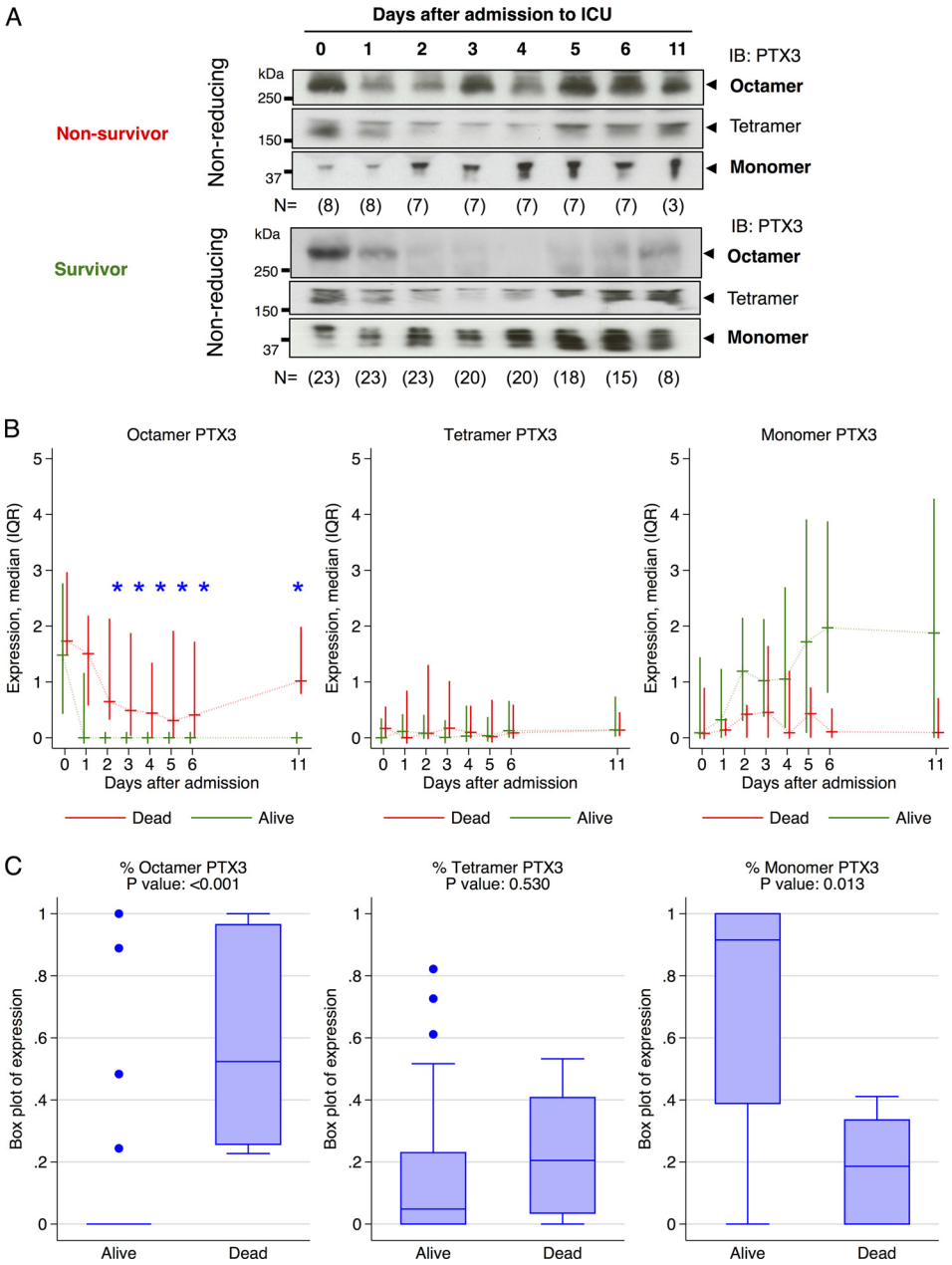

FIG. 5. **Association of PTX3 oligomerization with patient survival.** *A*, representative immunoblots of the development of the PTX3 oligomerization state with time after admission in a non-surviving sepsis patient (upper panel) and in a surviving sepsis patient (bottom panel). N-numbers corresponding to patient death or dropout are given for each time point. *B*, serum samples from 31 septic patients after admission to ICU (day 0) over a time course of 11 days were analyzed for PTX3 levels after albumin depletion. Monomeric, tetrameric, and octameric PTX3 levels were quantified for each patient and time point using Western immunoblot analysis performed under non-reducing conditions. Asterisks (*) denote statistically significant differences between patients who died and those who survived during the follow-up time (28 days); $p < 0.05$. *C*, distribution of PTX3 oligomer levels on day 2 post-admission to ICU compared between survivors and non-survivors.

PTX3 and Inflammation—Resolution of inflammation is not a passive process and requires stop signals (31). In severe sepsis, an uncontrolled inflammatory response to infection causes damage to and subsequent failure of organs such as the lungs, heart, and kidneys. The underlying mechanisms of AOF are not well understood, and no effective mediator-targeted therapies for established AOF are available (32). Medical care of patients combines prompt treatment with antibiotics and supportive care and often requires artificial organ support provided in an ICU. Numerous studies have tested novel therapeutics attempting to block key steps in the inflammatory processes associated with AOF. However, despite over 200 sepsis randomized controlled trials since 1992, no effective therapies exist. Most interventions have failed

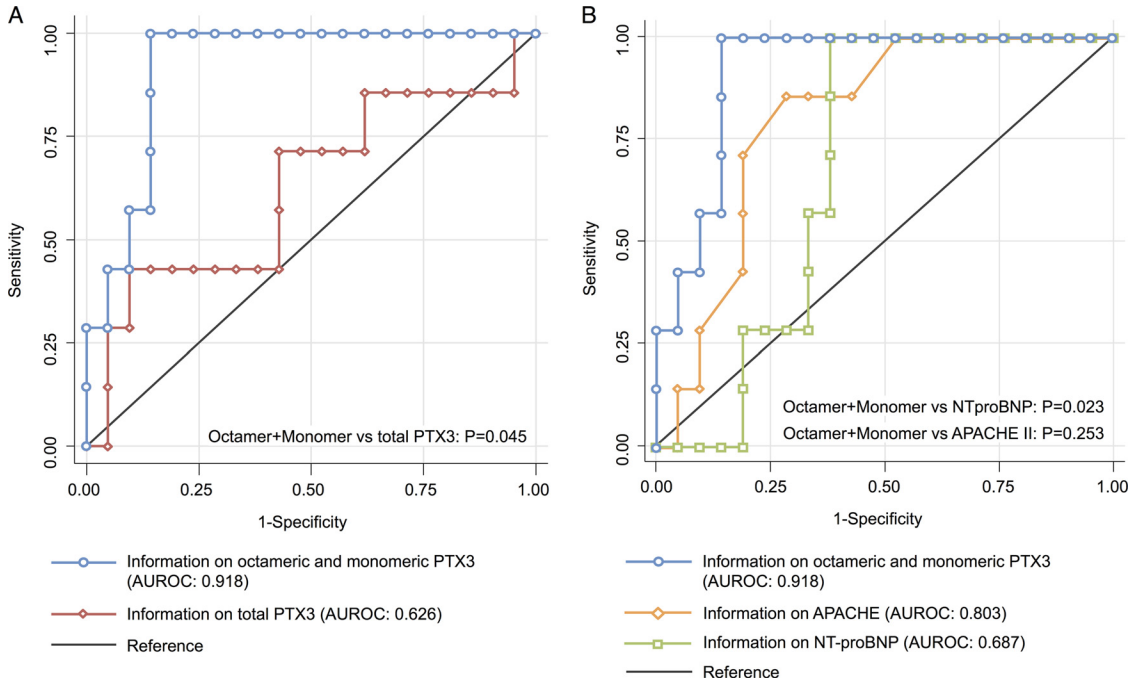

FIG. 6. **Comparison of the discriminatory power of octameric and monomeric PTX3 and other markers.** *A*, receiver operating characteristic curves of PTX3 measurements compared with total PTX3. Octameric and monomeric PTX3 levels at day 2 predicted the 28-day survival better than a model containing total PTX3 as measured by conventional ELISA (28 observations, area under the receiver operating characteristic curve (AUROC): 0.918 *versus* 0.626; *p* value: 0.045). *B*, receiver operating characteristic curves of PTX3 measurements compared with NT-proBNP and the clinical APACHE II score. Octameric and monomeric PTX3 levels at day 2 predicted the 28-day survival better than a model containing NT-proBNP (28 observations, AUROC: 0.918 *versus* 0.687; *p* value: 0.023) but failed to significantly outperform the APACHE II score in this patient cohort (28 observations, AUROC: 0.918 *versus* 0.803, $p = 0.25$).

when tested in rigorous trials (33). Previous anti-inflammatory interventions mainly targeted circulating inflammatory cells or inflammatory mediators (*i.e.* by dialysis). The observed retention of oxidized PTX3 in the Triton-insoluble fraction and the inverse correlation of circulating monomeric PTX3 with cardiac damage markers support the concept that inflammation and tissue damage may be perpetuated locally. Thus, in addition to targeting circulating mediators of inflammation, resolving the inflammation within the tissues might be a promising strategy in the prevention of AOF.

Clinical Significance—AOF in sepsis is common and is associated with high mortality, short-term morbidity, and significant chronic illness. Many biomarkers have been identified, but they lack specificity or sensitivity. Our tissue-based proteomics approach (34, 35) led to the novel observation that the oligomerization state of PTX3 could be a better prognostic biomarker in sepsis than total PTX3 as measured by conventional ELISA. Mechanistically, PTX3 oxidation may be linked to innate immunity and increased oxidative stress during inflammation (*i.e.* by the respiratory burst during neutrophil extracellular trap formation). Although levels of octameric PTX3 on admission day were not different between survivors and non-survivors, a dynamic change in the oligomerization state of PTX3 within the first 2 days might assist in identifying treatment response, or lack thereof, in patients with progressive illness or persistent organ dysfunction. A single biomarker, however, is unlikely to outperform the APACHE score, which consists of 12 variables (age, rectal temperature, mean arterial pressure, pH arterial, heart rate, respiratory rate, serum sodium, serum potassium, creatinine, hematocrit, leukocyte count, and the Glasgow Coma Scale).

Strengths and Limitations—ELISA technology is widely used in clinical diagnostics to detect total protein levels. In this work, we have demonstrated that the oligomerization state of circulating PTX3 might provide an important advantage over total PTX3 or cardiac damage markers in determining treatment response. Further studies in larger cohorts are required in order to confirm whether the oligomerization state of PTX3 is a superior surrogate end point for therapeutic interventions. As mediator molecules in the responses of the innate immune system, PTX3 multimers might be not only an indicator of but also a contributor to the deleterious host responses in sepsis. Whether this is a mechanism for the prolongation of tissue inflammation and progression to AOF awaits clarification in future studies (36).

CONCLUSIONS

An estimated 200,000 U.S. ICU patients die every year. Our findings suggest that the transformation of octameric to monomeric PTX3 in survivors might be a surrogate end point for the inflection point at which oxidative stress subsides and inflammation turns into resolution/repair. If sepsis patients at

risk of developing AOF could be identified early, this novel biomarker could help to "personalize" critical care medicine.

Acknowledgments—We thank Melanie Neumann and Kristin Hartmann (UKE HEXT core facility mouse pathology) for generating histology slides.

* F.C. was supported by an RCUK Fellowship, the DZHK (German Center for Cardiovascular Research), and the German Ministry of Research and Education (BMBF). P.W. was supported by a British Heart Foundation Ph.D. Studentship. M.M. is a Senior Fellow of the British Heart Foundation. The research was funded/supported by the National Institute of Health Research (NIHR) Biomedical Research Centre based at Guy's and St Thomas' NHS Foundation Trust and King's College London in partnership with King's College Hospital.

S This article contains supplemental material.

|||| To whom correspondence should be addressed: Prof. Manuel Mayr, King's British Heart Foundation Centre, King's College London, 125 Coldharbour Lane, London SE5 9NU, UK. Tel.: 44-0-20-7848-5132; Fax: 44-0-20-7848-5296; E-mail: manuel.mayr@kcl.ac.uk.

Disclosure: King's College has filed a patent application with regard to using oxidized PTX3 as a biomarker.

REFERENCES

1. Rittirsch, D., Flierl, M. A., and Ward, P. A. (2008) Harmful molecular mechanisms in sepsis. *Nat. Rev. Immunol.* **8,** 776–787
2. Anderson, N. L., and Anderson, N. G. (2002) The human plasma proteome: history, character, and diagnostic prospects. *Mol. Cell. Proteomics* **1,** 845–867
3. Anderson, L., and Hunter, C. L. (2006) Quantitative mass spectrometric multiple reaction monitoring assays for major plasma proteins. *Mol. Cell. Proteomics* **5,** 573–588
4. Jacquet, S., Yin, X., Sicard, P., Clark, J., Kanaganayagam, G. S., Mayr, M., and Marber, M. S. (2009) Identification of cardiac myosin-binding protein C as a candidate biomarker of myocardial infarction by proteomics analysis. *Mol. Cell. Proteomics* **8,** 2687–2699
5. Didangelos, A., Stegemann, C., and Mayr, M. (2012) The -omics era: proteomics and lipidomics in vascular research. *Atherosclerosis* **221,** 12–17
6. Mayr, M., Zampetaki, A., Willeit, P., Willeit, J., and Kiechl, S. (2013) MicroRNAs within the continuum of postgenomics biomarker discovery. *Arterioscl. Thromb. Vasc. Biol.* **33,** 206–214
7. Mayr, M., Zhang, J., Greene, A. S., Gutterman, D., Perloff, J., and Ping, P. (2006) Proteomics-based development of biomarkers in cardiovascular disease: mechanistic, clinical, and therapeutic insights. *Mol. Cell. Proteomics* **5,** 1853–1864
8. Abi-Gerges, N., Tavernier, B., Mebazaa, A., Faivre, V., Paqueron, X., Payen, D., Fischmeister, R., and Mery, P.-F. (1999) Sequential changes in autonomic regulation of cardiac myocytes after in vivo endotoxin injection in rats. *Am. J. Resp. Crit. Care Med.* **160,** 1196–120
9. Tavernier, B., Li, J. M., El-Omar, M. M., Lanone, S., Yang, Z. K., Trayer, I. P., Mebazaa, A., and Shah, A. M. (2001) Cardiac contractile impairment associated with increased phosphorylation of troponin I in endotoxemic rats. *FASEB* **15,** 294–296
10. Yin, X., Bern, M., Xing, Q., Ho, J., Viner, R., and Mayr, M. (2013) Glycoproteomic analysis of the secretome of human endothelial cells. *Mol. Cell. Proteomics* **12,** 956–978
11. Yin, X., Cuello, F., Mayr, U., Hao, Z., Hornshaw, M., Ehler, E., Avkiran, M., and Mayr, M. (2010) Proteomics analysis of the cardiac myofilament subproteome reveals dynamic alterations in phosphatase subunit distribution. *Mol. Cell. Proteomics* **9,** 497–509
12. Pavelka, N., Fournier, M. L., Swanson, S. K., Pelizzola, M., Ricciardi-Castagnoli, P., Florens, L., and Washburn, M. P. (2008) Statistical similarities between transcriptomics and quantitative shotgun proteomics data. *Mol. Cell. Proteomics* **7,** 631–644
13. Pavelka, N., Pelizzola, M., Vizzardelli, C., Capozzoli, M., Splendiani, A., Granucci, F., and Ricciardi-Castagnoli, P. (2004) A power law global error model for the identification of differentially expressed genes in microarray data. *BMC Bioinformatics* **5,** 203
14. Levy, M. M., Fink, M. P., Marshall, J. C., Abraham, E., Angus, D., Cook, D., Cohen, J., Opal, S. M., Vincent, J. L., and Ramsay, G. (2003) 2001 SCCM/ESICM/ACCP/ATS/SIS International Sepsis Definitions Conference. *Crit. Care Med.* **31,** 1250–1256
15. Bottazzi, B., Doni, A., Garlanda, C., and Mantovani, A. (2010) An integrated view of humoral innate immunity: pentraxins as a paradigm. *Annu. Rev. Immunol.* **28,** 157–183
16. Inforzato, A., Rivieccio, V., Morreale, A. P., Bastone, A., Salustri, A., Scarchilli, L., Verdoliva, A., Vincenti, S., Gallo, G., Chiapparino, C., Pacello, L., Nucera, E., Serlupi-Crescenzi, O., Day, A. J., Bottazzi, B., Mantovani, A., De Santis, R., and Salvatori, G. (2008) Structural characterization of PTX3 disulfide bond network and its multimeric status in cumulus matrix organization. *J. Biol. Chem.* **283,** 10147–10161
17. Bottazzi, B., Vouret-Craviari, V., Bastone, A., De Gioia, L., Matteucci, C., Peri, G., Spreafico, F., Pausa, M., D'Ettorre, C., Gianazza, E., Tagliabue, A., Salmona, M., Tedesco, F., Introna, M., and Mantovani, A. (1997) Multimer formation and ligand recognition by the long pentraxin PTX3. Similarities and differences with the short pentraxins C-reactive protein and serum amyloid P component. *J. Biol. Chem.* **272,** 32817–32823
18. Introna, M., Alles, V. V., Castellano, M., Picardi, G., De Gioia, L., Bottazzai, B., Peri, G., Breviario, F., Salmona, M., De Gregorio, L., Dragani, T. A., Srinivasan, N., Blundell, T. L., Hamilton, T. A., and Mantovani, A. (1996) Cloning of mouse ptx3, a new member of the pentraxin gene family expressed at extrahepatic sites. *Blood* **87,** 1862–1872
19. Lee, G. W., Goodman, A. R., Lee, T. H., and Vilcek, J. (1994) Relationship of TSG-14 protein to the pentraxin family of major acute phase proteins. *J. Immunol.* **153,** 3700–3707
20. Alles, V. V., Bottazzi, B., Peri, G., Golay, J., Introna, M., and Mantovani, A. (1994) Inducible expression of PTX3, a new member of the pentraxin family, in human mononuclear phagocytes. *Blood* **84,** 3483–3493
21. Breviario, F., d'Aniello, E. M., Golay, J., Peri, G., Bottazzi, B., Bairoch, A., Saccone, S., Marzella, R., Predazzi, V., Rocchi, M., Della Valle, G., Dejanna, E., Mantovani, A., and Introna, M. (1992) Interleukin-1-inducible genes in endothelial cells. Cloning of a new gene related to C-reactive protein and serum amyloid P component. *J. Biol. Chem.* **267,** 22190–22197
22. Daigo, K., Yamaguchi, N., Kawamura, T., Matsubara, K., Jiang, S., Ohashi, R., Sudou, Y., Kodama, T., Naito, M., Inoue, K., and Hamakubo, T. (2012) The proteomic profile of circulating pentraxin 3 (PTX3) complex in sepsis demonstrates the interaction with azurocidin 1 and other components of neutrophil extracellular traps. *Mol. Cell. Proteomics* **11,** M111.015073
23. Huttunen, R., and Aittoniemi, J. (2011) New concepts in the pathogenesis, diagnosis and treatment of bacteremia and sepsis. *J. Infect.* **63,** 407–419
24. Mauri, T., Bellani, G., Patroniti, N., Coppadoro, A., Peri, G., Cuccovillo, I., Cugno, M., Iapichino, G., Gattinoni, L., Pesenti, A., and Mantovani, A. (2010) Persisting high levels of plasma pentraxin 3 over the first days after severe sepsis and septic shock onset are associated with mortality. *Intensive Care Med.* **36,** 621–629
25. Uusitalo-Seppala, R., Huttunen, R., Aittoniemi, J., Koskinen, P., Leino, A., Vahlberg, T., and Rintala, E. M. (2013) Pentraxin 3 (PTX3) is associated with severe sepsis and fatal disease in emergency room patients with suspected infection: a prospective cohort study. *PLoS One* **8,** e53661
26. Wang, F., Wu, Y., Tang, L., Zhu, W., Chen, F., Xu, T., Bo, L., Li, J., and Deng, X. (2012) Brain natriuretic peptide for prediction of mortality in patients with sepsis: a systematic review and meta-analysis. *Crit. Care* **16,** R74
27. Knaus, W. A., Draper, E. A., Wagner, D. P., and Zimmerman, J. E. (1985) APACHE II: a severity of disease classification system. *Crit. Care Med.* **13,** 818–829
28. Silvestre, J., Povoa, P., Coelho, L., Almeida, E., Moreira, P., Fernandes, A., Mealha, R., and Sabino, H. (2009) Is C-reactive protein a good prognostic marker in septic patients? *Intensive Care Med.* **35,** 909–913
29. Bottazzi, B., Garlanda, C., Cotena, A., Moalli, F., Jaillon, S., Deban, L., and Mantovani, A. (2009) The long pentraxin PTX3 as a prototypic humoral pattern recognition receptor: interplay with cellular innate immunity. *Immunol. Rev.* **227,** 9–18
30. Dias, A. A., Goodman, A. R., Dos Santos, J. L., Gomes, R. N., Altmeyer, A., Bozza, P. T., Horta, M. F., Vilcek, J., and Reis, L. F. (2001) TSG-14 transgenic mice have improved survival to endotoxemia and to CLP-induced sepsis. *J. Leukoc. Biol.* **69,** 928–936

31. Li, Y., Dalli, J., Chiang, N., Baron, R. M., Quintana, C., and Serhan, C. N. (2013) Plasticity of leukocytic exudates in resolving acute inflammation is regulated by microRNA and proresolving mediators. *Immunity* **39,** 885–898
32. Marshall, J. C. (2003) Such stuff as dreams are made on: mediator-directed therapy in sepsis. *Nat. Rev. Drug Discov.* **2,** 391–405
33. Sweeney, D. A., Danner, R. L., Eichacker, P. Q., and Natanson, C. (2008) Once is not enough: clinical trials in sepsis. *Intensive Care Med.* **34,** 1955–1960
34. Didangelos, A., Yin, X., Mandal, K., Baumert, M., Jahangiri, M., and Mayr, M. (2010) Proteomics characterization of extracellular space components in the human aorta. *Mol. Cell. Proteomics* **9,** 2048–2062
35. Didangelos, A., Yin, X., Mandal, K., Saje, A., Smith, A., Xu, Q., Jahangiri, M., and Mayr, M. (2011) Extracellular matrix composition and remodeling in human abdominal aortic aneurysms: a proteomics approach. *Mol. Cell. Proteomics* **10,** M111.008128
36. Thiele, J. R., Habersberger, J., Braig, D., Schmidt, Y., Goerendt, K., Maurer, V., Bannasch, H., Scheichl, A., Woollard, K., von Dobschütz, E., Kolodgie, F., Virmani, R., Stark, G. B., Peter, K., and Eisenhardt, S. U. (2014) The dissociation of pentameric to monomeric C-reactive protein localizes and aggravates inflammation: in vivo proof of a powerful pro-inflammatory mechanism and a new anti-inflammatory strategy. *Circulation* **130,** 35–50